Hirosaki Med. J. 65：82—94, 2014

ORIGINAL ARTICLE

USEFULNESS OF ULTRAVIOLET-MICROSCOPIC SPECTROSCOPY ON UNSTAINED CELLS BY LIQUID-BASED CYTOLOGY FOR OBJECTIVE DIFFERENTIATION BETWEEN NON-CANCER FROM CANCER CELLS

Haruhiko Yoshioka[1)], Keita Hoshiai[1)], Toshiya Nakamura[2, 3)], Tatsusuke Sato[4)], Kiyotada Washiya[1)], and Jun Watanabe[1, 3)]

Abstract ***Object***: To investigate the usefulness of ultraviolet-microscopic spectroscopy (UV-MS) of unstained cells by liquid-based cytology (LBC) to objectively differentiate non-cancer from cancer cells. ***Study Design***: Cultured cells were used as the sample cells: 100 non-cancer cells and 200 cancer cells. The sample measurement region was a 166.4-μm^2 area in the nuclear region of sample cells. On UV-MS, data of 260, 280, 300, 320, and 340 nm were extracted from the transmittance spectrum of 260-350-nm ultraviolet (UV) wavelengths and analyzed. ***Result***: At a 300-nm UV wavelength, transmittances in non-cancer and cancer cells were 79.7 ± 5.0 and 64.1 ± 5.0%, respectively, being significantly lower in cancer cells ($P<0.01$). On discriminant analysis, a linear discriminant function: Z=0.61 x transmittance (300 nm) - 44.02, was obtained. When the function value is positive and negative, the cell is judged as a cancer or non-cancer cell, respectively. The accuracy of this linear discriminant function was 96.3%, sensitivity was 98.0%, specificity was 93.0%. ***Conclusions***: UV-MS on unstained cells by LBC yields an objective value to discriminate non-cancer from cancer cells. Since LBC is a sample processing procedure which will be increasingly used in the future, we are planning to further investigate its applicability to clinical specimens based on this study.

Hirosaki Med. J. 65：82—94, 2014

Key words: Ultraviolet-microscopic spectroscopy; Liquid-based cytology; Discriminant analysis; Unstained cells.

原 著

がん細胞と非がん細胞の鑑別における無染色の液状処理細胞診を用いた紫外顕微分光法の有用性

吉岡治彦[1)]　星合桂太[1)]　中村敏也[2, 3)]　佐藤達資[4)]
鷲谷清忠[1)]　渡邉純[1, 3)]

抄録　非がん細胞とがん細胞の客観的な鑑別指標を得るため，無染色の液状処理細胞診(Liquid-based Cytology; LBC法)を材料とした紫外顕微分光法(Ultraviolet-Microscopic Spectroscopy; UV-MS法)の有用性を検証した．材料は非がん細胞100個，がん細胞200個の合計300個の培養細胞である．UV-MS法において測定領域は核内領域の166.4 μm^2 (12.9 μm×12.9 μm)，解析データは紫外線波長260～350 nmの透過率スペクトルから260 nm, 280 nm, 300 nm, 320 nm, 340 nmのデータを抽出した．その結果，紫外線波長300 nmにおいて非がん細胞の透過率は79.7 ± 5.0%，がん細胞は64.1 ± 5.0%であり，がん細胞は有意($P<0.01$)に低くなった．さらに判別分析の結果，判別関数　Z=0.61×transimittance(300 nm) - 44.02　判別的中率: 96.3%，係数のp値: < 0.01以下で有意に強く判別に関わることが分かった．

無染色のLBC法を用いたUV-MS法は，非がん細胞とがん細胞の鑑別に客観的な価値を与えることが分かった．LBC法は世界的に需要の高い処理となっており，本研究を基盤に臨床材料に応用できるか更に検討を進めたい．

弘前医学　65：82—94, 2014

キーワード：紫外顕微分光法；液状処理細胞診；判別分析；無染色細胞.

[1)] Department of Pathologic Analysis, Division of Medical Life Sciences, Hirosaki University Graduate School of Health Sciences
[2)] Department of Biomedical Sciences, Division of Medical Life Sciences, Hirosaki University Graduate School of Health Sciences
[3)] Reserch Center for Biomedical Sciences, Hirosaki University Graduate School of Health Sciences
[4)] CLARO, Inc.
Correspondence: H. Yoshioka
Received for publication, November 8, 2013
Accepted for publication, December 25, 2013

[1)] 弘前大学大学院保健学研究科医療生命科学領域病態解析科学分野
[2)] 弘前大学大学院保健学研究科医療生命科学領域生体機能科学分野
[3)] 弘前大学大学院保健学研究科生体応答科学研究センター
[4)] 株式会社クラーロ
別刷請求先：吉岡治彦
平成25年11月8日受付
平成25年12月25日受理

Introduction

Liquid-based cytology (LBC) has recently been used frequently in the cytology field, and it is no exaggeration to say that it is a revolution in sample processing. As the characteristics of this method, it detects low-grade squamous intraepithelial lesion (LSIL) or more severe lesions at a high sensitivity and accuracy, microscopic observation is readily performed because the cell distribution is homogenous and stainability is consistent, and the time required for observation is shortened because the visual field is limited[1-6]. In addition, it has become possible to additionally perform immunocytochemistry and gene analysis after making a diagnosis of the cell morphology using the residual sample in the LBC solution vial, showing that the clinical advantage of LBC can widely contribute to Ki- 67 antibody (MIB-1) index-based malignancy judgment, the detection of Human papillomavirus (HPV), and judgment of the effect of molecular targeted therapy of Human epidermal growth factor receptor 2 (HER-2) and Epidermal growth factor receptor (EGFR), in addition to cytology. As disadvantages of LBC, rounding, atrophy, and paling of the nuclei readily occur due to liquefaction of the cell morphology, compared to the conventional sample processing method, and reduction of necrotized materials and inflammatory cells are observed in the background[7-12] . Therefore, establishment of specific judgment criteria for LBC and those of adenocarcinoma cells with poor nuclear atypia is needed.

Ultraviolet-microscopic spectroscopy (UV-MS) is a spectrum analysis method widely used in absorption spectrophotometry[13] and fluorescence spectroscopy[14] in the organic chemistry field. Aqueous solution is used as a solvent in many samples of UV-MS, and only a few studies have directly used cells as a sample. In recent studies, Zeskind et al. [15] and Cheung et al. [16] used unfixed viable cultured cells as samples, showing that the analysis of intracellular nucleic acids and proteins is possible by measuring the absorbance at 260- and 280-nm UV wavelengths.

The objective of this study was to perform UV-MS analysis of cultured cells processed by LBC, which has not been performed in previous studies, and investigate objective differentiation between non-cancer and cancer cells. The future objective of this study is to apply this procedure to clinical cases difficult to differentiate, and establish an objective index to identify cancer cells.

Materials and Methods

Cell samples by LBC

Six types of cultured cell were used as samples: human skin fibroblasts (NHDF)[17] and African green monkey kidney cells (COS-7)[18] as non-cancer cell-derived cells, and human lung cancer cells (A549)[19], human breast cancer cells (MCF-7)[20], human colon cancer cells (LS-180)[21], and human gastric cancer cells (KATOIII)[22] as cancer cells.

Trypsin-treated cultured cells (1 x 10^6 /ml) of each cell line in 1 ml of culture medium were combined with 9 ml of LBC solution, ThinPrep PreservCyt (ThinPrep, HOLOGIC Japan, Tokyo, Japan), to prepare 10 ml of suspension, and the suspension was kept standing overnight.

Samples were processed for UV-MS as follows: From a suspension of each sample, 5-ml aliquots were distributed into 15 ml tube, centrifuged at 1,500 rpm for 2 minutes using Cyto-Tec Cytocentrifuge (Model CF-127, Sakura, Tokyo, Japan), and directly smeared on a quartz glass (Technical, Aomori, Japan). The smear was subjected to wet fixation in 95% ethanol for 30 minutes, and sealed with a quartz cover glass (Technical) using a glycerin

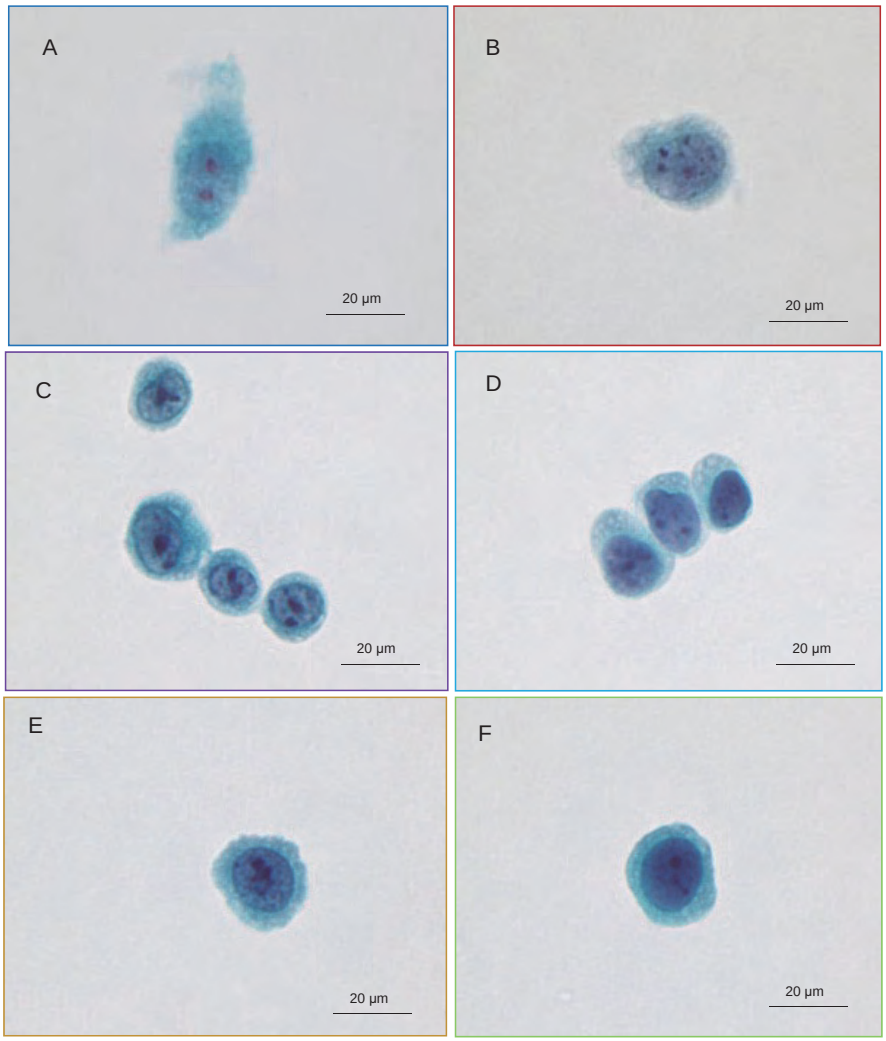

Figure 1 Papanicolaou-stained cells by LBC
Non-cancer cells: NHDF (a), COS-7 (b), Cancer cells: LS-180 (c), MCF-7 (d), A549 (e), KatoIII (f)

mounting agent without staining.

For conventional Papanicolaou staining, samples were similarly processed by LBC. The procedure differed thereafter: Conventional slide glasses for light microscopy (FINE FROST, MATUNAMI, Tokyo, Japan) were used for the direct smearing of samples centrifuged at 1,500 rpm for 2 minutes (Cyto-Tec). After direct smearing, the slides were subjected to wet fixation in 95% ethanol for 30 minutes and then stained by conventional Papanicolaou. The stained cells are shown in Figure 1.

Lambert-Beer law

This UV-MS involves the application of light absorption and absorption spectroscopy used in the analytical chemistry field to LBC. The principle of light absorption in analytical chemistry, the Lambert-Beer law, is as follows:

The principle of absorbance measurement is measurement of the light absorbed when a monochromatic light passes through a sample. When a sample with a concentration, c (c *mM*), is added into an absorption cell, a monochromatic light with an intensity of I_0 passes through an optical path length, l, and the

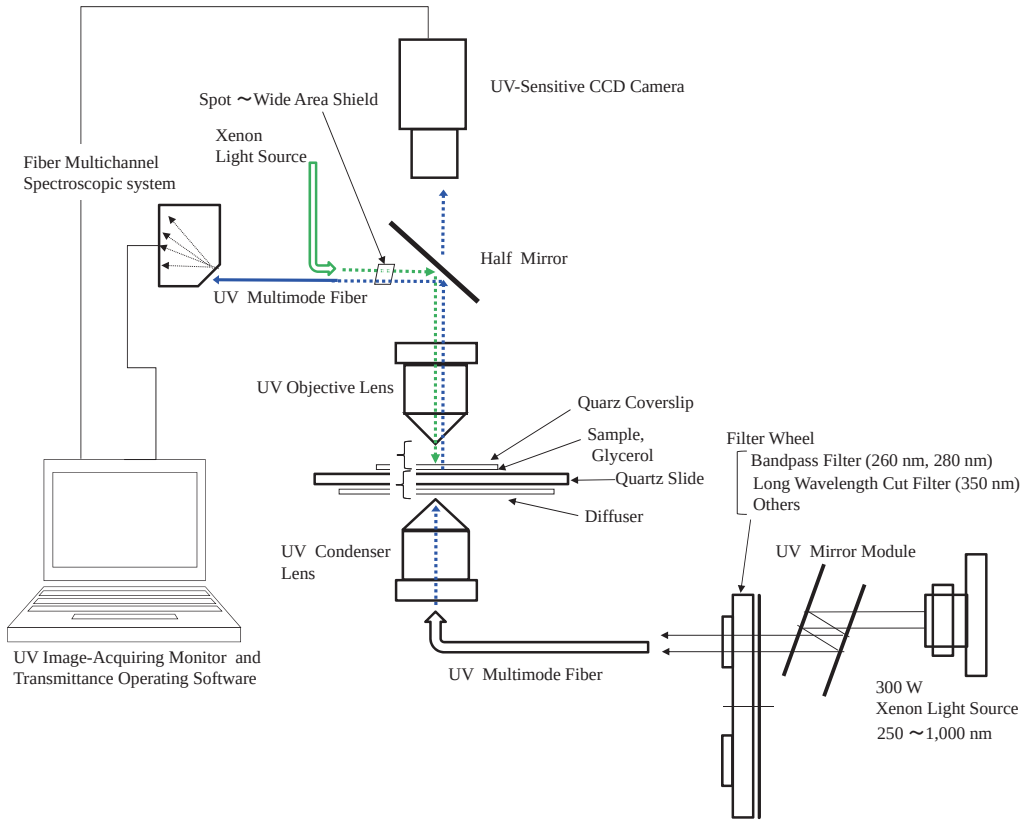

Figure 2 Schematic diagram of UV-MS system

intensity becomes I. $\frac{I}{I_0}$ is termed transmittance and expressed as T. When this is presented as a percentage, it is termed the percent transmittance and expressed as T%. $-\log\frac{I}{I_0}$ is termed absorbance and expressed as A. Accordingly:

$$A = -\log T = -\log\frac{I}{I_0} = \varepsilon cl \qquad (1)$$

ε is termed the extinction coefficient. Absorbance is proportional to the passing distance of light and concentration of the solution. This is the Lambert-Beer law.

With minor exceptions, the sum of concentrations of different chemical species is measured as absorbance. Thus, there is additivity, and the absorbance of a sample containing n absorption activities is presented as follows:

$$A = -\log\frac{I}{I_0} = dl\sum_{i=1}^{n}\varepsilon_i c_i \qquad (2)$$

Using multifunctional software for spectroscopy (Ocean Photonics, Japan), transmittance, T%, was measured on assumption that this equation is true.

UV-MS system

A schema of the UV-MS system is shown in Figure 2.

Light source (MAX-302, ASAHIBUNKOU, Tokyo, JAPAN)

For the light source lamp, a 300-W xenon lamp with an emission spectrum over a broad continuous wavelength range (250-1,000 nm) was used. The durability of the lamp is 500 hours, and this study was performed within this period. For the cooling system of the light source lamp, a forced air-cooling and exhaust

system was employed, which improved the continuous irradiation durability of the light source and variation without reducing the light quantity, even though irradiation at 100% was continued for 2 hours. The quantity of the light could be changed in 1% increments from 5 to 100%. A low light quantity (30%) was adopted because the stability of the light source at this level is optimal and cellular damage is minimal.

For the intermediate filter of the light source, a UV-mirror module was set to select UV wavelengths from the broad continuous wavelength range of the light source. Since a high-performance cold mirror is used in the UV-mirror module, unnecessary heating is completely inhibited, and the stray light level is extremely low, as characteristics of the UV-mirror module.

For the second filter in the optical path in the light source device, MAX-302, a 350-nm-wavelength cut-off filter was used. A characteristic of the 350-nm-wavelength cut-off filter is its capability of simultaneously measuring the transmittances of continuous wavelengths (250-350 nm). The light quantity condition for transmittance measurement is identical for all continuous wavelengths, and this is its major characteristic. The disadvantage of this filter is its low contrast in absorption images compared to that using a band-pass filter. The specificity is high in absorption images acquired using a band-pass filter because the images are acquired at a specific band wavelength. In contrast, the band width of the output wavelength with a long wavelength cut-off filter is large, which increases absorbed substances and widens the absorption region, reducing image specificity

Light from the light source, MAX-302, passes through a quartz fiber cable, enters a quartz condenser lens in the UV-MS device, and condenses. The light enters from below a sample slide set on the stage. The light is partially absorbed by sample cells and the remaining light penetrates them. The light penetrating the sample enters and is magnified by a quartz objective lens, and enters the half mirror. The light is then divided equally in two by the half mirror. One division enters a UV-sensitive CCD camera for acquiring UV images, and the other enters a quartz cable connected to a spectrophotometer. Using the half mirror, observation of UV absorption images and measurement of the transmittance of each wavelength in the sample region can be simultaneously performed in real time.

Spectroscope (Figure 2)

Light penetrating the sample region enters a high-sensitivity fiber multichannel spectroscope (QE65000, Ocean Photonics, Tokyo, Japan) through the half mirror and quartz fiber cable. Reflection grating was employed for continuous spectrum spectroscopy using this spectroscope. The photo detector is an electronic cooling back-illuminated FFT-CCD area image sensor, and the number of effective pixels was 1,024 x 58/24.5 μm square. The range of wavelength measurement of this spectroscope is 200-1,100 nm and dependent on 14 types of grating. For the spectroscope analysis software, OP wave+ (Ocean Photonics) was used.

Sample region to detect spectra

The measurement range is set so as to allow the transmitted light to pass through the nuclear region. In the UV-MS system, the range was set by adjusting the Spot-Wide Area Shield (Figure 2). Area Shield was positioned along the quartz fiber between the half mirror and spectroscope. Area Shield adjusts the light by blocking it with 4 shields in 4 directions. The measurement range was set as follows: Light in the quartz fiber connected to the spectroscope was passed in a direction opposite to normal (Figure 2, a green arrow). The light output in

the opposite direction while adjusting the Area Shield position was reflected by the half mirror and descended. It was then epi-illuminated on the slide glass set on the stage and reflected. The light reflected by the slide glass ascended to the objective lens, passed through the half mirror, and was output into the image-acquiring camera. The target sample area can be confirmed in this glass-reflected image. The magnification of the objective lens to acquire data was 10 times. For observation of nuclear findings and confirmation of the nucleoli, a 40x objective lens was used. When fine re-adjustment of the area was necessary, Area Shield was adjusted. The measurement area can involve a single focal point or a large tissue, but the area is a square or rectangle because the light is shielded in 4 directions, and so it is not sufficiently applicable for curved regions, which is a disadvantage of Area Shield.

The sample measurement area (166.4 μm^2 (12.9 x 12.9 μm)) was the same in all cells in this study. The measurement area mostly covered the nucleus, but, strictly, it does not cover the total volume of the nucleus.

Basic setting for UV-MS measurement

The spectroscope was set as follows: After turning on the main unit power, the spectrum integration time, mean number of measurements, and number of smoothing operations were set at 100 msec, once, and 20, respectively, on the setup screen of multifunctional software for spectroscopy, OP wave+. The spectroscope was warmed up for 15 minutes to stabilize the cooling motor. Calibration of the wavelength for UV transmittance and noise correction were performed as follows: In the calibration, the UV-MS conditions for transmittance measurement and imaging were adjusted. It is not necessary to calibrate the wavelength in each measurement. It was performed once every time the sample slide was changed. The dark signal was saved while shielding the light entering the spectroscope to eliminate negative dark signals. This procedure cancels out electric noise of the spectroscopy system. The xenon light source was turned on and warmed up for 15 minutes. Then, a reference serving as the standard for transmittance measurement was established. The reference served as the standard 100% transmittance.

Measurement method using the transmittance measurement mode

After the basic setting of the spectroscope described above, a sample slide was set on the stage of the microscope, and the mode of the multifunctional software for spectroscopy OP wave+ was switched to that for transmittance measurement. To control transmittance measurement of samples, the following procedure was performed for each sample. Measurements of 0 and 100% transmittance control areas were set at sites very close to the sample cell, which eliminated the transmittance of substances around the sample cell and enabled setting the 100% transmittance baseline.

The measurement area was then moved from the control to the sample measurement site while observing the UV absorption image. A sample cell was selected while confirming that the measurement area was included in the nuclear region, the cell was not overlapped with other cells, and the nuclei was not atrophied, swollen, or crushed due to cell degeneration. In transmittance measurement of each sample, a Bit-Map UV absorption images of the measurement region were acquired using imaging software (Basico, CLARO). From the UV transmittance spectrum obtained using OP wave+, the measured transmittance values of UV wavelengths of 260, 280, 300, and 320 nm were saved as Excel data. The number of measured cells was 50 in each cell line, with 300 cells in total: 100 non-cancer and 200 cancer

cells.

Statistical analysis

In non-cancer and cancer cells, the UV transmittance was determined at 20-nm intervals in the continuous spectrum from 260 to 340 nm, and the means and standard deviations were determined. The normality of the distribution in the non-cancer and cancer cells was analyzed at each UV wavelength using the Shapiro-Wilk test. When the distribution was not normal, the significance of differences between the non-cancer and cancer cells was analyzed using the Mann-Whitney U test. These analyses were performed using the statistical analysis software SPSS 16.0j.

The accuracy of discrimination of the non-cancer and cancer cells was investigated employing discriminant analysis using multivariate analysis software, Mulcel [23]. The objective of discriminant analysis is to prepare a rule for discrimination. For example, in discriminant analysis using distance, when values of variates (n=p): X1, X2, ・・・ Xp, are observed in 2 groups of samples, a rule is prepared to determine which group an observed value, X, belongs to. Designating the mean vector of the distributions of the 2 populations as μ1 and μ2, respectively, and the variance-covariance matrices as Σ1 and Σ2, respectively, the distance between the center of gravity (mean vector) and X is determined to include X in the closer group. For the distance, Mahalanobis' generalized distance, calculated in consideration of the variance of and correlation between variates, was used:

$$\Delta_k^2 = {}^t(x-\mu_k)\sum_k{}^{-1}(x-\mu_k) \quad (k=1, 2) \qquad (3)$$

On the assumption that the 2 groups are normal populations of multiple variates and their variance-covariance matrices are equal, using the observed value as the estimate of the population, the coordinates of the centers of gravity of the groups, $\overline{X_1}$ and $\overline{X_2}$, are the means of variates X_1, X_2, ⋯, X_p, the variance-covariance matrix is the pooled variance-covariance matrices of the 2 groups, S_1 and S_2,

$$S = \frac{(n_1-1)S_1 + (n_2-1)S_2}{n_1+n_2-2}$$

(n_1 and n_2 represent the numbers of data of the groups, respectively). Mahalanobis' generalized distance is calculated from these using the equation below:

$$D_k^2 = {}^t(X-\overline{X_k})S^{-1}(X-\overline{X_k}) \quad (k=1, 2) \qquad (4)$$

When $D_2^2 \geq D_1^2$, X is judged as belonging to Group 1.

When $D_2^2 < D_1^2$, X is judged as belonging to Group 2.

Designating $Z = D_2^2 - D_1^2$, discrimination is determined based on the positivity or negativity of Z in this rule.

A test of homogeneity was performed (Box's M test) to investigate whether the variance of variates X_1, X_2, ⋯, X_p and correlations between variates are equal between the 2 groups. When these are equal, Z is presented as the following linear equation:

$$Z = a_0 + a_1X_1 + a_2X_2 + \ldots + a_pX_p \qquad (5)$$

Z of equation (5) is termed the linear discriminant function. The level of contribution of each variate to the obtained linear discriminant function is judged by testing the coefficient of equation (5), *ai*. Null hypothesis, H_0: $ai=0$, and alternative hypothesis, H_1: $ai \neq 0$, were tested, for which the statistics using squared Mahalanobis' distance (4) followed the F distribution at one degree of freedom (1, n_1+n_2-p-1). From the results of discrimination, the accuracy (= number of true positive cells + true negative cells/total number), sensitivity (=number of true positive cells/number of diseased cells), and specificity (=number of true negative cells/number of non-diseased cells) were determined.

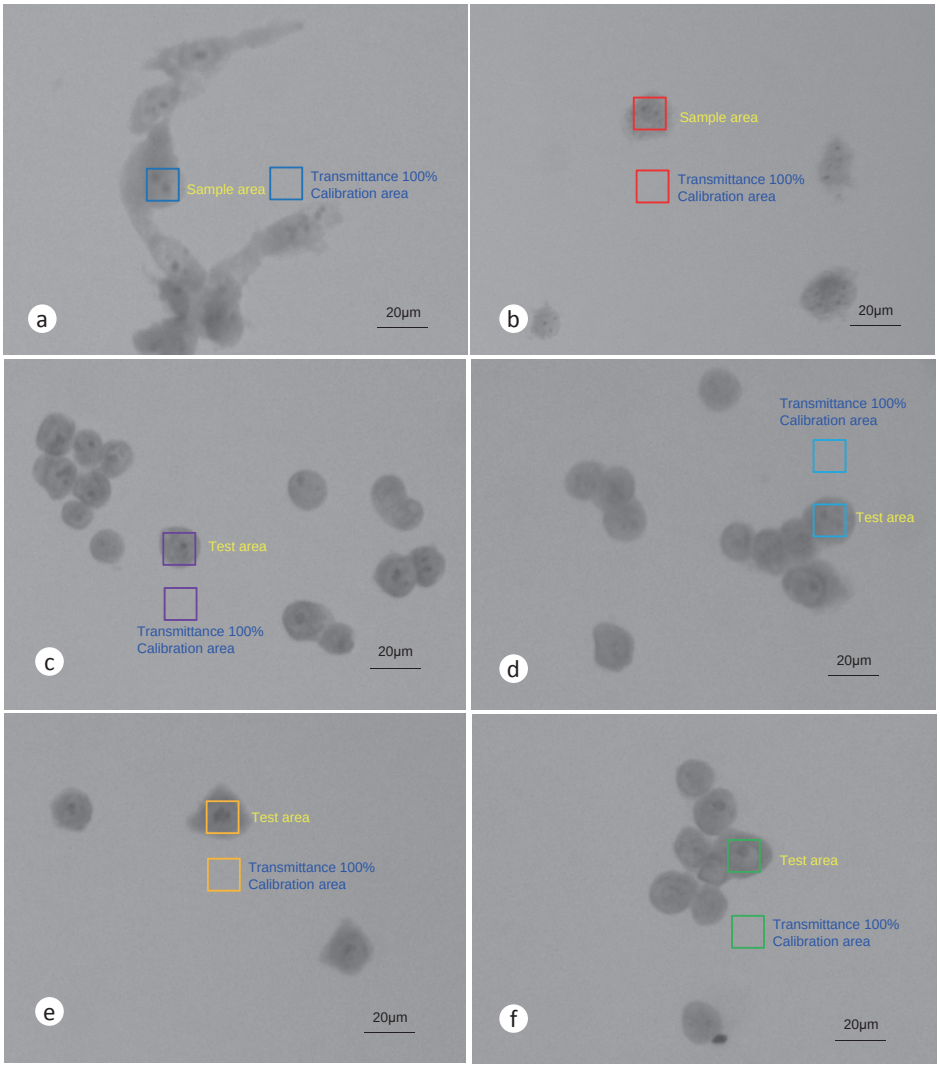

Figure 3 UV absorption images of unstained cells acquired using a 350-nm-wavelength cut-off filter
Non-cancer cells: NHDF (a), COS-7 (b), Cancer cells: LS-180 (c), MCF-7 (d), A549 (e), KatoIII (f)

Results

UV (250-350 nm) absorption images acquired using a 350-nm-wavelength cut-off filter

Figure 3 shows the UV (250-350 nm) absorption images acquired using the 350-nm-wavelength cut-off filter (scale: 20 μm). Squares represent measurement areas (166.4 μm^2 (12.9 x 12.9 μm)). The sample nuclear measurement and 100% transmittance reference regions are presented (the colors of the lines correspond to those of outline of the light microscopic images in Figure 1). The shade and light of the absorption images of the cells represent high and low absorption of 250-350-nm UV light, respectively. In all cells, absorption was noted in not only the chromatin but also nuclear matrices and nucleolar regions in the nuclei, but it was difficult to identify a characteristic feature of cancer cells in these absorption images.

UV (250-350 nm) absorption spectrum of each cell

The mean and standard deviation of

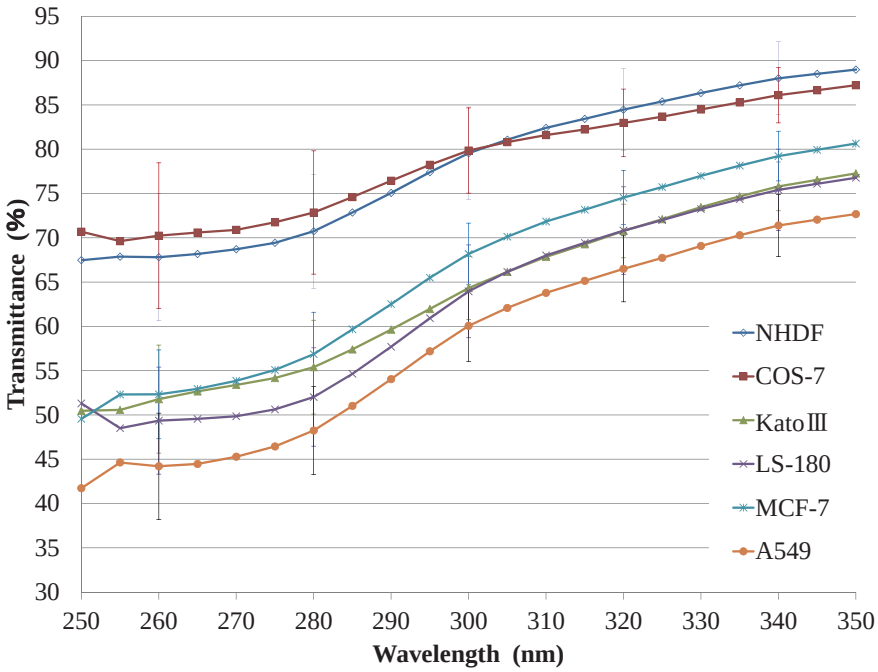

Figure 4 Comparison of the UV transmittance of unstained cultured cells (n=300) measured using a 350-nm-wavelength cut-off filter
Non-cancer cells: NHDF, COS-7. Cancer cells: LS-180, MCF-7, A549, KatoIII.

Table 1 Comparison of the transmittance measured using the UV-MS between non-cancer and cancer cells

Wavelength (nm)	Transmittance (mean±SD)%		P-value
	Non-cancer cells (n=100)	Cancer cells (n=200)	
260	69.0 ± 7.9	49.4 ± 6.6	< 0.01
280	71.8 ± 6.8	53.1 ± 6.1	
300	79.7 ± 5.0	64.1 ± 5.0	
320	83.7 ± 4.3	70.7 ± 4.7	
340	87.1 ± 3.8	75.5 ± 4.5	

transmittance measured in 50 cells of each cell line are shown in Figure 4. The transmittance was lower in cancer (n=200) than in non-cancer (n=100) cells at all wavelengths, and the waveforms of the spectra were similar, but slight concavo-convex differences were noted.

The significance of differences in the transmittances of 260, 280, 300, 320, and 340 nm between non-cancer and cancer cells was analyzed (Table 1). Firstly, at each wavelength, the normality of the distribution of non-cancer and cancer cell preparations was investigated using the Shapiro-Wilk test. At all wavelengths, the significance level was $p<0.05$ in at least one of the 2 groups, showing a distribution deviating from normal. Thus, analysis was performed using a nonparametric method, Mann-Whitney U test (Table 1), and the p-value was less than 0.01 at all wavelengths, showing that the transmittances of all wavelengths of 260, 280, 300, 320, and 340 nm were significantly lower in cancer than in non-cancer cells.

Since significant differences between the non-cancer and cancer cells were detected by UV-

Table 2 Homogeneity of variance-covariance matrices of non-cancer and cancer cells and discrimination function formula for each wavelength

Test wavelength (nm)	Homogeneity of variance-covariance matrix (p-value)	Linear discriminant function	Test of coefficient of linear discriminant function (p-value)
260	0.05	Z=0.39 x T (260 nm) − 23.21	< 0.01
280	0.22	Z=0.46 x T (280 nm) − 28.69	
300	0.99	Z=0.61 x T (300 nm) − 44.02	
320	0.31	Z=0.62 x T (320 nm) − 47.64	
340	0.07	Z=0.64 x T (340 nm) − 51.91	

T: transmittance

Table 3 Evaluation of cancer cell discrimination in LBC-processed cells using the UV-MS

Test wavelength (nm)	Evaluation of discriminant analysis (n=300)		
	Accuracy (%)	Sensitivity (%)	Specificity (%)
260	93.7	96.5	88.0
280	93.0	96.0	87.0
300	96.3	98.0	93.0
320	94.7	96.0	92.0
340	92.7	92.5	93.0

MS, the discrimination function to distinguish the 2 cell groups was determined using a multivariate analysis method, discriminant analysis. At each test wavelength employed for the discrimination (260, 280, 300, 320, and 340 nm), the homogeneity of the variance-covariance matrix between the non-cancer and cancer cell groups was investigated using Box's M test (Table 2). At all test wavelengths, the p-value was greater than 0.05, showing that there was no difference in the variance-covariance matrix between the non-cancer and cancer cells (i.e., the variance-covariance matrices were equal). Thus, multivariate analysis (discriminant analysis) was performed using the linear discriminant function, equation (5). When the coefficient of the linear discriminant function was tested, the p-value of the coefficient of discrimination function was less than 0.01 at all test wavelengths, showing significance at a level of 1% (Table 2). Therefore, it was clarified that the coefficient of each linear discriminant function is closely involved in the discrimination. The discrimination using the wavelength spectrum and UV-MS was useful to differentiate LBC-processed cultured cancer cells. The accuracy of discrimination using the linear discriminant function at each wavelength was investigated (Table 3). The accuracy was the highest at 300 nm.

The linear discriminant function of the transmittance of the 300-nm wavelength was established as follows:

Z=0.61 x transmittance (300 nm) - 44.02 (6)

The accuracy of this linear discriminant function was 96.3%, and the sensitivity and specificity were 98.0 and 93.0%, respectively. It was shown that when the transmittance of 300 nm in sample X is assigned in this formula, and a positive value is obtained, the cell is judged as cancerous, and when it is negative, the cell is judged as non-cancerous.

Discussion

The usefulness of UV-MS of LBC-processed unstained cells for objective differentiation between non-cancer and cancer cells was investigated, and a discrimination function with accuracy, sensitivity, and specificity of 96.3,

98.0, and 93.0%, respectively, was obtained (6). The parameter of this discrimination was the transmittance of 300-nm-wavelength UV light. To our knowledge, there has been no previous report combining the following 3 points concerning a method to discriminate between non-cancer and cancer cells: 1) A parameter serving as an objective index of UV-MS was identified, 2) UV-MS could be applied for cytology, and 3) cell materials processed with LBC could be used for UV-MS.

Lakowicz et al. [14] reported phenylalanine (260 nm), tyrosine (275 nm), tryptophan (295 nm), and NADH (340 nm) as substances with specific UV absorbance. In our study, UV transmittance was lower in cancer than in non-cancer cells, suggesting that cancer cells contain more UV-absorbing substances. Although no specific substance could be identified in this study, it was strongly suggested that various UV-absorbing materials described above were mixed. Organic chemical[14] and mass spectrometric analyses[13] using cell materials are necessary.

Zeskind et al. [15] and Cheung et al. [16] reported UV-MS using unfixed cultured viable cells as samples. They demonstrated the intracellular nucleic acid and protein levels by analyzing the pixel intensity in absorption images of cultured viable cells at UV wavelengths of 260 and 280 nm. We used our original device developed for this UV-MS. The advantage of this microscope is its capability of simultaneously observing the UV absorption image and measuring the UV spectrum. The fact that investigation can be performed while observing the UV absorption image may facilitate the application of morphological information acquired in the cytology field for differentiation between non-cancer and cancer cells. Investigation of differences between the UV absorption and Papanicolaou- and Giemsa-stained images may be useful to improve the accuracy of diagnostic discrimination in the future. However, this device has a disadvantage: adjustment of the sample measurement area using shields in 4 directions. Since the shape of the measurement area is mainly square or rectangular, spectra corresponding to round and oval areas cannot be acquired, remaining as a task of device development in the future. But we confirmed that there was no significant difference of the ratio of the measured field to the nuclear region between non-cancer and cancer cells using the images of Papanicolaou staining samples.

For sample preparation for UV-MS, we could demonstrate the usefulness of applying LBC. Zeskind et al. [15] and Cheung et al. [16] pointed out cytopathy due to the toxicity of UV light for unfixed cultured viable cells of samples. In our study, the UV transmittance was measurable even though UV light was irradiated for a time sufficient to observe UV absorption images, and this may be due to the fixation of cells in LBC. In cytology mainly using images of Papanicolaou-stained cells, wet fixation with 95% ethanol solution is essential. Processing by LBC has recently been frequently used. Significant discrimination between non-cancer and cancer cells was possible in the LBC-processed samples, and this may promote the application of UV-microscopic spectroscopy for clinical cytology. This study using cultured cells as samples is a basic study of the application for clinical cytology, and we are planning to advance the study using clinical samples from actual patients.

Acknowledgments

This study was supported by a Grant for Hirosaki University Institutional Research (2010-2012). The authors are grateful to Drs Koichi Ito, Kosuke Kasai, Manabu Nakano of Hirosaki University Graduate School of Health Sciences for preparing cell lines.

Disclosure Statement

None of the authors has any conflict of interest

References

1) Kuramoto H, Iwami Y, Sugimoto N, Kato C, Sugahara T, Iida M. Application of a New Liquid-Based Procedure (TACAS) for the Screening of Cervical Cancer: A Preliminary Study. Acta Cytol 2012;56:74-9.

2) Nance KV. Evolution Pap testing at a community hospital: a ten-year experience. Diagn Cytopathol 2007;35:148-53.

3) Akamatsu S, Himeji Y, Ikuta N, Shimagaki N, Maruoka H, Kodama S. Satisfactoriness and disease detection in the screening specimens of cervical cancer - comparison between liquid-based and conventional methods. J Jpn Soc Clin Cytol 2008;47:420-4.

4) Hutchinson ML, Isenstein LM, Goodman A, Hurley AA, Douglas KL, Mui KK, Patten FW, et al. Homogenous sampling accounts for the increase diagnostic accuracy using the ThinPrep® Processor. Am J Clin Pathol 1994;101:215-9.

5) Lee KR, Ashfaq R, Birdsong GG, Corkill ME, Mclntosh KM, Inhorn SL. Comparison of conventional Papanicolaou smears and fluid-based, thin-layer system for cervical cancer screening. Obstet Gynecol 1997;90:278-84.

6) Hatch KD, Sheets E, Kennedy A, Ferris DG, Darragh T, Twiqqs L. Multicenter direct-to-vial evaluation of a liquid-based Pap test. J Lower Genit Tract Dis 2004;8:308-12.

7) Watanabe J, Nishimura Y, Tsunoda S, Kawaguchi M, Okayasu I, Kuramoto H. Liquid-based preparation for endometrial cytology - Usefulness for predicting the prognosis of endometrial carcinoma preoperatively. Cancer (Cancer Cytopathol) 2009;117:254-63.

8) Kim GE, Kweon SS, Lee JS, Lee JH, Nam JH, Choi C. Quantitative assessment of DNA methylation for the detection of cervical and endometrial adenocarcinomas in liquid-based cytology specimens. Anal Quant Cytol Histol 2012;34:195-203.

9) Spathis A, Kottaridi C, Georgoulakis J, Foukas P, Panayiotides L, Peros G, Karakitsos P. Cell cycle analysis of colorectal brushings collected in liquid-based cytology. Anal Quant Cytol Histol 2011;33:29-35.

10) Malapelle U, de Rosa N, Rocco D, Bellevicine C, Crispino C, lllino A, Piantedosi FV, et al. EGFR and KRAS mutations detection on lung cancer liquid-based cytology: a pilot study. J Clin Pathol 2012;65:87-91.

11) Vocaturo A, Novelli F, Benevolo M, Piperno G, Marandino F, Cianciulli AM, Merola R, et al. Chromagenic in situ hybridization to detect HER-2/*new* gene amplification in histological and ThinPrep®-processed breast cancer fine-needle aspirates: A sensitive and practical method in the trastuzumab era. Oncologist 2006;11:878-86.

12) Sartelet H, Lagonotte E, lorenzato M, Duval I, Lechki C, Rigaud C, Cucherousset J, et al. Comparison of liquid based cytology and histology for the evaluation of HER-2 status using immunostaining and CISH in breast carcinoma. J Clin Pathol 2005;58:864-71.

13) Meier H. UV/Vis Spectroscopy. In: Hesse M, Meier H, Zeeh B. Spectroscopic Methods in Organic Chemistry. 2nd ed. New York: Thieme; 2008. p.1-32.

14) Lakowicz JR. Fluorophres. In: Lakowicz JR. Principles of Fluorescence Spectroscopy. 3rd ed. Baltimore: Springer; 2009. p63-95.

15) Zeskind BJ, Jordan CD, Timp W, Trapani L, Waller G, Horodincu V, Ehrlich DJ, et al. Nucleic acid and protein mass mapping by live-cell deep-UV microscopy. Nat Methods 2007;4:567-9.

16) Cheung MC, Evans JG, McKenna B, Ehrlich DJ. Deep UV mapping of intracellular protein and nucleic acid in femtograms per pixel. Cytometry Part A 2011;79A:920-32.

17) Nakamura T, Takagaki K, Shibata S, Tanaka k, Higuchi T, Endo M. Hyaluronic-acid-deficient extracellular matrix induced by addition of 4-methylumbelliferone to the medium of cultured human skin fibroblasts. Biochem Biophys Res Commun 1995;208:470-5.

18) Okabe K, Inada N, Gota C, Harada Y, Funatsu T, Uchiyama S. Intracellular temperature mapping with a fluorescent polymeric thermometer and fluorescence lifetime imaging microscopy. Nat Commun 2012;3:705.

19) Carterson AJ, Höner zu Bentrup K, Ott CM, Clarke MS, Pierson DL, Vanderburg CR, Buchanan KL, et al. A549 Lung Epithelial Cells Grown as Three-Dimensional Aggregates: Alternative Tissue Culture Model for Pseudomonas aeruginosa Pathogenesis. Infect Immun 2005;73:1129-40.

20) Karimi-Busheri F, Rasoul-Nia A, Mackey AR, Weinfeld M. Senescence evasion by MCF-7 human breast tumor-initiating cells. Breast Cancer Res 2010;12:R31.

21) McCool DJ, Forstner JF, Forstner GG. Regulated and unregulated pathways for MUC2 mucin secretion in human colonic LS180 adenocarcinoma cells are distinct. Biochem J 1995;312:125-33.

22) She JJ, Zhang PG, Wang X, Che XM, Wang ZM. Side population cells isolated from KATO III human gastric cancer cell line have cancer stem cell-like characteristics. World J Gastroenterol 2012;18:4610-7.

23) Yanai H. Discriminant analysis. In: Yanai H. Practical Mutivariate Analysis Greate Utilities on Exel. Tokyo: OMS publshing Inc.; 2010. p.101-114.